Theoret. chim. Acta (Berl.) 18, 184—192 (1970)

Topography of the Electron Density in Pyrophosphate Bonds

DONALD B. BOYD
The Lilly Research Laboratories, Indianapolis

Received March 10, 1970

Contour maps of the electron density in the phosphorus-oxygen bonds of inorganic ortho- and pyro-phosphate molecules and in the biologically important nucleotide adenosine-5′-diphosphate (ADP) are presented. The densities and overlap populations calculated from approximate molecular orbital methods are used to explain the nature of the so-called "energy-rich" phosphate bond. The P 3*d* orbitals are able to contribute more to the π bond strength of the terminal P–O bonds than to the P–OP bonds. Equations are introduced for calculating changes in valence electron distributions brought about by molecular formation and for comparing Mulliken populations with spatial distributions of electrons.

Die Elektronendichte in den Phosphor-Sauerstoff-Bindungen anorganischer Ortho- und Pyro-Phosphat-Moleküle sowie in dem biologisch wichtigen Nukleotid Adenosin-5′-Diphosphat (ADP) werden in Höhenliniendiagrammen dargestellt. Die Dichten und Überlappungspopulationen, die nach der MO-Methode näherungsweise berechnet wurden, werden benutzt, um die Natur der „energiereichen" Phosphat-Bindung zu erklären. Die P 3*d* Orbitale tragen mehr zu der π-Bindungsstärke der endständigen P–O-Bindung als zur P–OP-Bindung bei. Für die Berechnung von Änderungen in der Valenzelektronen-Verteilung durch Molekülbildung sowie für den Vergleich der Mulliken-Population mit der räumlichen Elektronenverteilung werden Beziehungen abgeleitet.

Cartes de contour de densité électronique sur les liaisons phosphore-oxygène dans les molécules d'ortho et de pyrophosphate inorganiques et dans la molécule d'importance biologique de diphosphate-5′-d'adénosine. Les densités et les populations électroniques calculées dans le cadre de méthodes d'orbitales moléculaires approchées sont utilisées pour expliquer la nature de la liaison phosphate dite «riche en énergie». Les orbitales 3*d* de P sont à même de contribuer plus énergiquement à la force de la liaison π des liaisons P–O terminales qu'à celle des liaisons P–OP. On introduit des équations pour calculer les modifications dans la distribution des électrons de valence provoquées par la formation de la molécule et pour comparer les populations de Mulliken avec les distributions spatiales des électrons.

Introduction

The pyrophosphate bond, P–OP, occurs extensively in biological systems and is perhaps best recognized as an element of adenosine-5′-triphosphate (ATP). The pyrophosphate bond can provide, through its hydrolysis in ATP, the important driving force for many endergonic reactions of the cell. Advancing sophistication in computer programming has recently permitted molecular orbital calculations of a semiempirical nature on ATP and related large molecules [1, 2]. These calculations led to an examination of two electronic factors which for many years have been associated with the so-called "high-energy" phosphate bond: 1) opposing resonance, which is the existence of more delocalization energy in the products of hydrolysis than is possible in the reactants, and 2) electrostatic repulsions between the atoms of the polyphosphate chain. Simple considerations of valence structures and π-electron Hückel calculations were the only previous

attempts to examine these qualitive concepts (for a review of earlier work, [1–3]). The recent calculations [1, 2] took into account the three-dimensional nature of the molecules and involved the valence-electron extended Hückel (EH) and the all-electron NEMO II [4] methods. The size of the molecules involved in a study of the pyrophosphate bond precludes, for the present, any *ab initio* approaches to obtaining more accurate wave functions. Nevertheless, the approximate wave functions [1, 2] were found to be qualitatively consistent with a wide range of properties of the molecules. Thus, it is desirable to bring to bear further computational techniques on these wave functions in order to extract information which will supplement the scant experimental data on the electronic structures of the inorganic and biochemical phosphates.

We propose to examine the detailed distribution of electrons in molecules with the P–OP bond, $H_4P_2O_7$, $HP_2O_7^{3-}$, and ADP^{3-}, by calculating electron density contour maps [5, 6]. In light of the similarity of the triphosphates and pyrophosphates and in consideration of the computer times involved, only the pyrophosphates are studied here. Studied for comparison is orthophosphoric acid H_3PO_4, which is relatively small and hence relatively likely to be subjected to rigorous SCF calculations. In addition to computing total electron densities from the EH and NEMO II wave functions, difference density maps are also generated. The latter are contour plots of the molecular density minus the spherically symmetric atomic densities placed at the atomic positions of the molecule. Difference maps show the build-up of density in bonding regions, the creation of lone pair lobes, and other polarizations brought about by molecular formation. In the case of the NEMO II densities the reference atomic densities are the minimum Slater basis set, ground state, SCF atomic orbitals. The use of these orbitals, which have the same exponents as used in the MO calculations [1], is expected to yield difference maps bearing some resemblance to results from more accurate wave functions [5]. Difference maps involving the EH densities are obtained from $\Delta D(\boldsymbol{r}) = \sum_{p,\, q \neq p} D_{pq}\chi_p(\boldsymbol{r})\chi_q(\boldsymbol{r}) + \sum_p [D_{pp} - N(p)]\chi_p(\boldsymbol{r})\chi_p(\boldsymbol{r})$, where the sums are over valence (Slater-type) orbitals $\chi_p(\boldsymbol{r})$, D_{pq} is the density matrix element evaluated for N valence electrons, $\sum_{i=1}^{N} C_{pi}C_{qi}$, and $N(p)$ is the occupation number of each valence orbital in the ground state, infinitely separated, neutral atoms. The subtraction of $N(p)$ follows because the occupation numbers are equal to the diagonal, atomic density matrix elements as calculated within the EH framework. Plots of the total valence-electron density do not have the usual features of all-electron density maps, especially near and at the nuclei [5, 7]. Consequently, only difference maps are presented for the EH wave functions.

Features of the Electron Density Maps

We begin by discussing the electron density computed from the all-electron wave functions for H_3PO_4 (Figs. 1, 2) and $H_4P_2O_7$ (Figs. 3–6). The total density maps (Figs. 1, 3) reveal the general shape and size of the molecules. The effects of bond formation are more clearly shown in the difference maps, where charge build-ups in the σ bond regions of P=O, P–O, and O–H are apparent and in

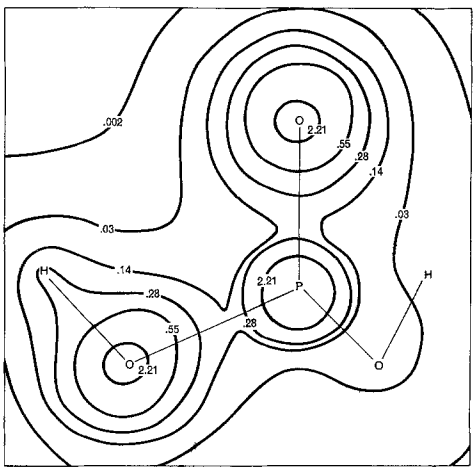

Fig. 1

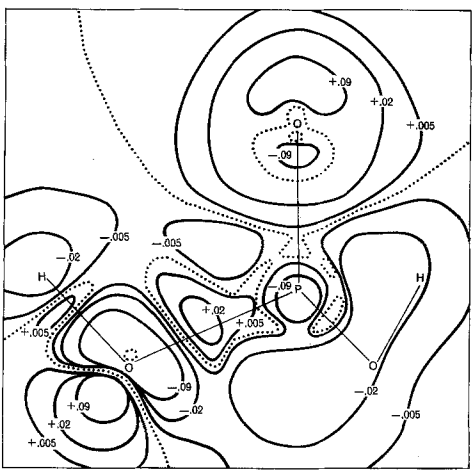

Fig. 2

Fig. 1. Total density map of H_3PO_4 computed from the NEMO II wave function. The density is computed in the plane of O=P−O−H with the projections of the other two P−O−H bonds shown on the right. All figures report densities in atomic units and cover an area of 4×4 Å. Densities at the nuclei in the order O= P−O−H are, respectively, 305.32, 2264.64, 304.45, and 0.46

Fig. 2. Difference density map of H_3PO_4, analogous to Fig. 1, with densities at the O=P−O−H nuclei of −2.08, −5.50, −2.95, and −0.12. Nodes are denoted by dotted lines

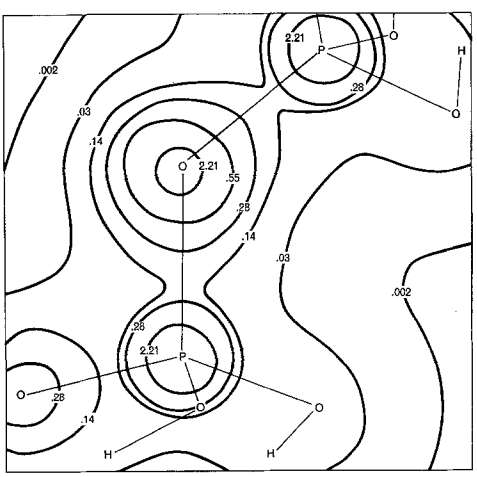

Fig. 3

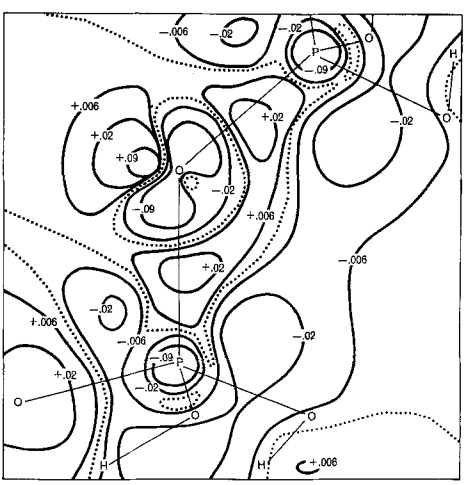

Fig. 4

Fig. 3. Total density map of $H_4P_2O_7$ computed from the NEMO II wave function in the plane of P−O−P. Densities are 2264.5 at the P nuclei and 303.63 at the bridge O

Fig. 4. Difference density map of $H_4P_2O_7$, analogous to Fig. 3, with densities of −5.6 at each P nucleus and −3.78 at the bridge O

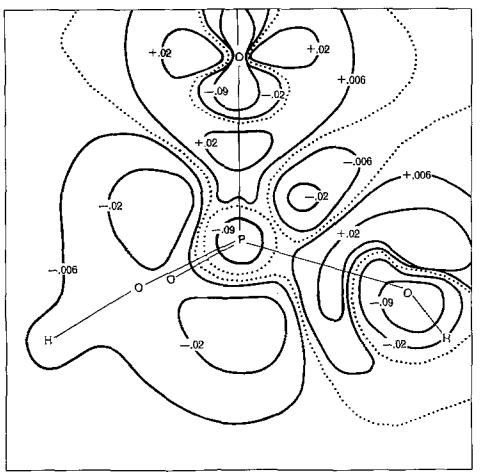

Fig. 5

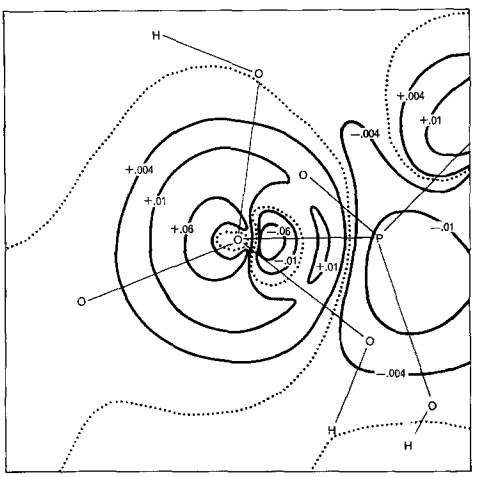

Fig. 6

Fig. 5. Difference density map of $H_4P_2O_7$ with the plane of calculation perpendicular to P–O–P plane and containing one P–OP bond. The other P lies off the map at the top. The O nucleus at the right lies about 0.2 Å from the plane of calculation

Fig. 6. Density difference map of $H_4P_2O_7$ with the plane of calculation passing through the bridge O and perpendicular to one P–OP bond, so that the projection of one P nucleus falls on the bridge O at the center of the map

the π region (off the internuclear axis) of the P=O bond in H_3PO_4. Lone pair densities appear as nubs over the ends of the terminal P=O bonds and as lobes on the nonbonded sides of the protonated and bridging oxygens. Compensating for these charge accumulations are losses from the immediate vicinity of the nuclei and on the nonbonded sides of phosphorus. These same general features are also found with *ab initio* wave functions on small molecules [5]. The lone pair density on the bridge oxygen extends both above and below the P–O–P plane (Fig. 6), corresponding to the out-of-plane O 2*p* orbital having a greater population [1] than either of the in-plane 2*p* orbitals. Furthermore, the bridge oxygen lone pair density, which is due mainly to the character of the two highest occupied MO's, is smaller than at any of the protonated oxygens, and this is in line with the larger net atomic charges on the latter atoms.

The difference maps for the ions of biological interest $HP_2O_7^{3-}$ and ADP^{3-} (Figs. 7–11) are quite dissimilar in appearance to the difference maps just discussed (Figs. 4–6). Contributing to the disparities are the different approximations involved in the calculations, the nature of the EH densities of not showing any polarizations of the core electrons [5], and the fact that the electrons in anions are more diffuse than in neutral molecules [5]. However, the features which are common in both the EH and NEMO II maps are the ones which are considered significant. Important to our later discussion, the formation of lone-pair build-ups on the oxygens is quite similar to that noted before. One also notes that charge distribution in the phosphate chain of ADP^{3-} appears to be not greatly affected by the esterification.

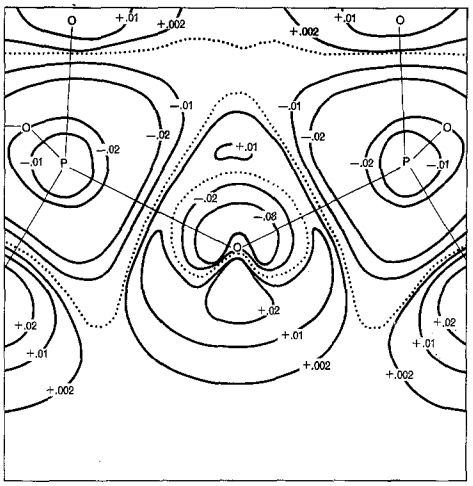

Fig. 7

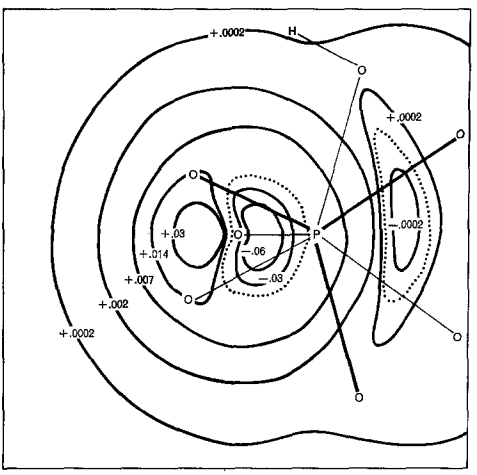

Fig. 8

Fig. 7. Difference density map of $HP_2O_7^{3-}$ computed from the EH wave function. The map gives the density in the P–O–P plane, where the densities are about −0.001 at the P nuclei and −0.016 at the bridge O. The protonated phosphate end lies at the left

Fig. 8. Difference density map of $HP_2O_7^{3-}$, analogous to Fig. 7, but in the plane passing through the bridge O (at the center of the map) and bisecting the P–O–P bond angle. The projections of the P–O bonds of the unprotonated phosphate group are drawn in heavy lines

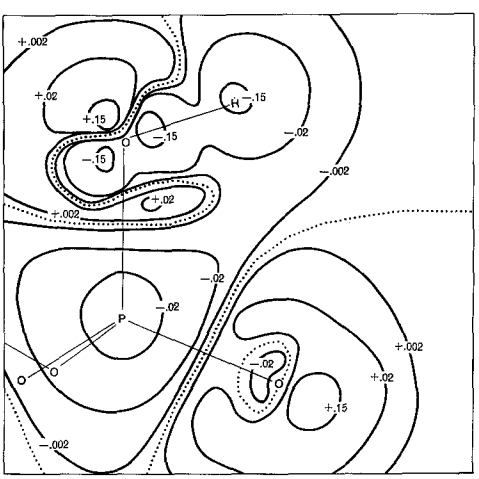

Fig. 9

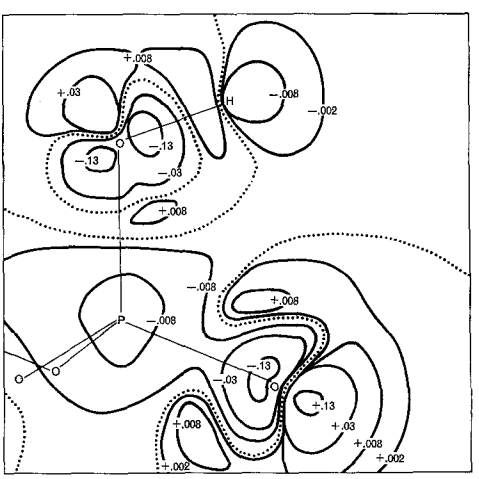

Fig. 10

Fig. 9. Difference density map of $HP_2O_7^{3-}$ in the plane of the shortest terminal bond and the protonated P–O bond. The proton also lies in this plane. The other phosphate group lies off the map at the left. Densities at the nuclei of O=P–O–H are −0.010, −0.001, −0.015, and −0.289

Fig. 10. Difference map of $HP_2O_7^{3-}$ in the same plane as in Fig. 9, but with $N(p)$ taken to be the orbital populations in the molecule. Densities at the O=P–O–H nuclei are −0.011, −0.001, −0.014, and −0.039

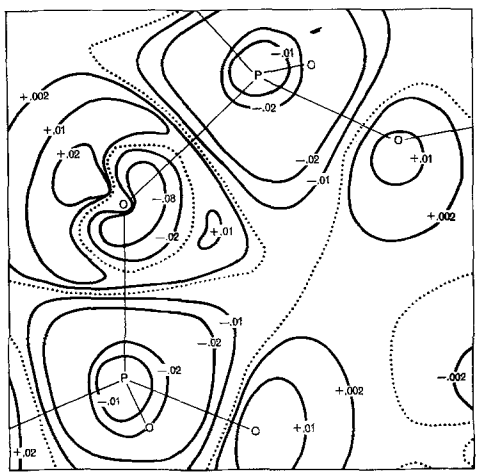

Fig. 11. Difference density map of the pyrophosphate chain of ADP^{3-} in the P–O–P plane. The P_α phosphate group (at the top) is connected to the nucleoside moiety which lies off the map at the right

Contrasting with Fig. 2, the EH density (Fig. 9) fails to show any σ bond density for the O–H bond because the EH wave function puts too much charge in the O $2p$ orbital perpendicular to the P–O–H plane. However, the population analysis of the EH MO's [2] gives a normal overlap population for the O–H bond. Other studies [8] indicate the EH densities do show σ density accumulations for C–H bonds, which are less ionic than O–H bonds.

The Mulliken population analysis [9] can itself be analyzed in the following manner. One might expect that if the population analysis is distributing the electrons among the basis functions in the manner described by a wave function, and if a difference function is computed by setting $N(p)$ equal to the orbital populations (total gross populations of the AO's [9]) derived from the *molecular* wave function, then the density differences should be zero or at least of small magnitude. A plot (Fig. 10) of such a difference function shows the peaks and valleys are not greatly leveled out from the ordinary difference map (Fig. 9). When integrated over all space the difference function plotted in Fig. 10, $\sum_{p,q} D_{pq}(\chi_p\chi_q - S_{pq}\chi_p\chi_p)$, gives zero, unlike the $\Delta D(r)$ function of Fig. 9 which integrates to the ionic charge on the molecule because of using neutral reference atomic densities. Fig. 10 shows where and to what extent the orbital populations do not represent the spatial distribution of electrons. It is noted that the anisotropic populations assigned to the p and d orbitals do not fully simulate the directional nature of the lone pairs.

Chemical Implications of the Charge Distributions

The population analysis of the MO wave functions of the polyphosphates [1, 2] gave the bridge oxygens a negative net atomic charge. However, as lucidly illustrated in the figures, the electron density responsible for this negative charge is in the lone pairs lobes, which are directed away from the P–P axis. The

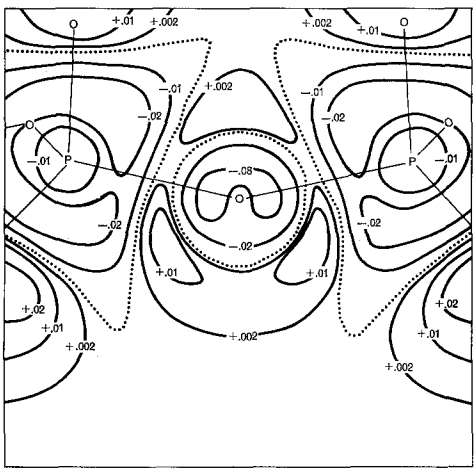

Fig. 12. Difference density map of $HP_2O_7^{3-}$ with a P–OP bond length of 1.5027 Å. Densities at the nuclei in the P–O–P plane are −0.001 at the P's and −0.023 at the bridge O

phosphorus atoms bear a positive charge [1, 2]. Thus, the stability of the phosphate chain is affected by a low concentration of electrons along the backbone of the chain [3]. The charge accumulations on the periphery of the chain will increase its rigidity against twisting, as well as influencing its reactivity [3]. Crystal structural data on the polyphosphates usually indicate an extended conformation. The presence of a metal ion, such as in biological systems, however, can result in conformational changes [10].

The bonding in the pyrophosphate bond is further explored by computing the EH energy [2] of the system while varying the position of the bridge oxygen along the two-fold symmetry axis of the pyrophosphate moiety and keeping the rest of the geometry [11] of $HP_2O_7^{3-}$ fixed. The limitations of EH theory are known [12] in regard to its ability to predict bond lengths and angles. Thus, it is not surprising that EH theory gives the optimum P–OP distance at about 1.51 Å. As the P–OP length is varied from 1.70 Å to 1.4624 Å (linear P–O–P) the P–OP overlap population increases from 0.88 to 1.15; also the net charges on the phosphorus atoms become progressively less positive and the charge on the bridge oxygen goes from −0.23 to +0.14. The migration of electron density away from the bridge oxygen is also seen in Fig. 12, which shows that the lone pair density is dissipated into the regions nearer the P nuclei due to the shorter P–OP distances.

Significant to understanding the nature of the so-called "high-energy" phosphate bond, it is found that the P–OP overlap population is less than the terminal P–O value when both bonds are given the same length. For convenience we will discuss the results calculated at 1.5027 Å (Fig. 12) because this is equal to the experimental distance [11] of one of the terminal P–O bonds. (Bond distances are not really significant to four decimal places, but for consistency with the calculations we will use four). The 1.5027 Å P–OP distance corresponds to a bent P–O–P angle of 153.4°, whereas the experimental values [11] are 1.612 Å and 130.2°. The tetrahedral-like hybridization at phosphorus is preserved

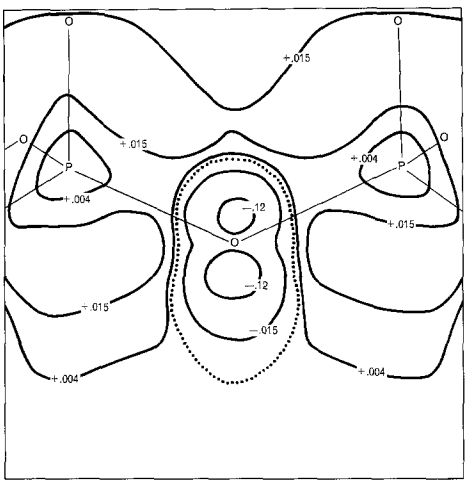

Fig. 13

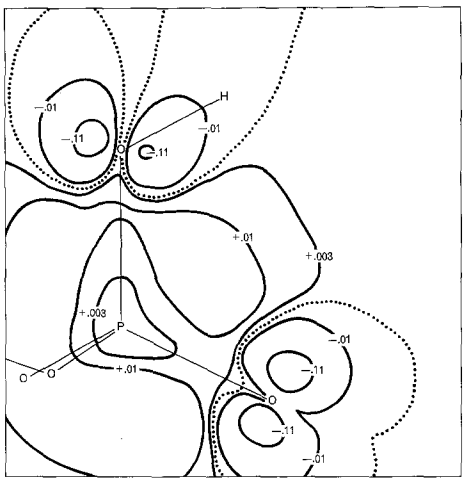

Fig. 14

Fig. 13. Difference map of $HP_2O_7^{3-}$ in the same plane as Fig. 7 showing the change in the molecular EH density brought about by including P 3*d* orbitals in the basis set

Fig. 14. Difference map of $HP_2O_7^{3-}$, analogous to Fig. 13, but in the same plane as Fig. 9

at the calculated equilibrium geometry because the average bond angle between the bridge and terminal oxygens (105.6°) is nearly equal to the experimental value (105.8°). However, no lengthening of the terminal P–O bonds has been included to compensate [13] for the shorter P–OP bonds. At 1.5027 Å, n(P–OP) is 1.12 and n(P–O) is 1.39. The fact that the EH calculations indicate the pyrophosphate bond is weaker than the terminal P–O bond gives some quantitative meaning to the concept of opposing resonance. Separating the σ and π overlap populations with respect to the individual bond axes indicates that the difference in overlap populations is mainly a π-electron effect (which might not be readily apparent from comparing the P–OP bond of Fig. 12 with the P=O bond of Fig. 9). The σ contributions to these overlap populations are similar (0.67 and 0.71 for the P–OP and P–O bonds at 1.5027 Å, respectively), whereas the π contributions are quite different (0.45 and 0.68). The interactions of the 3*d* orbitals account for 0.15 of the difference in π overlap populations. Contributions from orbitals in the P–O–P plane are comparable to those perpendicular to this plane.

The same picture emerges if one stretches one of the P–O bonds of the unprotonated terminus of $HP_2O_7^{3-}$ while holding the rest of the geometry fixed. At 1.6122 Å, the stretched bond has an overlap population of 1.20, whereas n(P–OP) at this distance is 0.98 in normal $HP_2O_7^{3-}$. The σ contributions are 0.63 to P–OP and 0.66 to P–O, and the π contributions are 0.35 and 0.54, respectively. The 3*d* orbitals contribute 0.12, or roughly two-thirds, of the difference in π overlap populations. It is therefore clear on the basis of these calculations that more $d_\pi - p_\pi$ bonding is possible in the P–O bonds than in the P–OP bonds. The reason for this is simply that the terminal oxygens have available more electrons for filling MO's which possess P $3d_\pi$ + O $2p_\pi$ character than do the bridge oxygens. The electrons of the bridge oxygens must be shared between

the two phosphorus atoms and hence cannot "back-bond" to either effectively. The molecule can gain stability by using the 3*d* orbitals to a greater extent in the terminal bonds, thereby causing these bonds to be shorter than the pyrophosphate bonds.

The "backbonding" effect permitted by the 3*d* orbitals can be pictured by subtracting the molecular density computed from the EH wave function without 3*d* orbitals from the one with them (Figs. 13, 14). Positive contours correspond to regions of $HP_2O_7^{3-}$ gaining density when 3*d* orbitals are included in the basis set. The results of this computer experiment are, of course, dependent on the parameters [2] used to calculate the EH MO's, and also the results are less accessible to experimental verification than some of the maps presented before. Nevertheless, the gross features of Fig. 13 and 14 can be taken to indicate the electron-accepting property of the 3*d* orbitals. Without 3*d* orbitals, the charge separations are unreasonably large (net charge on P is greater than +2), and the phosphorus-oxygen bonds are all weakened. With 3*d* orbitals, electron density is pulled out of the toroidal $2p_\pi$ orbital region around each oxygen. The inclusion of the 3*d* orbitals increases n(P–O) the most and n(P–OP) the least. This result reinforces the observation made above that the terminal P–O bonds can and do have greater $d_\pi - p_\pi$ bonding than any of the P–OP bonds. In conclusion then, structural features of the polyphosphates and the unique role of the "high-energy" phosphate bond in biological systems stem in part from the properties afforded by the 3*d* orbitals of phosphorus.

References

1. Boyd, D. B.: Theoret. chim. Acta (Berl.) **14**, 402 (1969).
2. — Lipscomb, W. N.: J. theoret. Biology **25**, 403 (1969).
3. Pullman, B., Pullman, A.: Quantum Chemistry, Chapter 7, New York: Interscience Publishers 1963.
4. Boyd, D. B., Lipscomb, W. N.: J. chem. Physics **48**, 4955 (1968).
5. — J. chem. Physics **52**, 4846 (1970).
6. — J. Amer. chem. Soc. **91**, 1200 (1969).
7. Hermann, R. B., Culp, H. W., McMahon, R. E., Marsh, M. M.: J. Med. Chem. **12**, 749 (1969).
8. Hoffmann, R., Boyd, D. B., Goldberg, S. Z.: J. Amer. chem. Soc. **92**, 3929 (1970).
9. Mulliken, R. S.: J. chem. Physics **23**, 1833 (1955).
10. Sundaralingam, M.: Biopolymers **7**, 821 (1969); Kennard, O., Isaacs, N. W., Coppola, J. C., Kirby, A. J., Warren, S., Motherwell, W. D. S., Watson, D. G., Wampler, D. L., Chenery, D. H., Larson, A. C., Kerr, K. A., Riva Di Sanseverino, L.: Nature **225**, 333 (1970).
11. McDonald, W. S., Cruickshank, D. W. J.: Acta crystallogr. **22**, 43 (1967).
12. Hoffmann, R.: J. chem. Physics **39**, 1397 (1963); Tetrahedron **22**, 521 (1966).
13. Cruickshank, D. W. J.: J. chem. Soc. (London) **1961**, 5486.

Dr. D. B. Boyd
The Lilly Research Laboratories
Eli Lilly and Company
Indianapolis, Indiana 46206, USA